ORIGINAL ARTICLE

ScienZTech

INTERNATIONAL JOURNAL OF NOVEL TRENDS IN PHARMACEUTICAL SCIENCES

Published by ScienzTech Publication Journal Home Page: www.scienztech.org/ijntps

In silico molecular docking studies and ADME/T analysis of Some Flavonoids against the target of Mpro in COVID-19

Kaviarasu J*, Suresh Kumar CA, Naimuddeen N

Department of Pharmaceutical chemistry, Aadhibhgawan College of Pharmacy, Rantham, Thiruvannamalai-604407, Tamilnadu, India

Article History:

Received on: 03 May 2020
Revised on: 14 Jun 2020
Accepted on: 25 Jun 2020
Published on: 10 Jul 2020

Volume: 10 Issue: 2

Keywords:

6LU7,
flavonoids,
COVID19,
catechin,
molecular Docking

ABSTRACT

COVID-19 may be a devastating global pandemic round the world. While the bulk of infected cases appear mild, in some cases, individuals present respiratory complications with possible severe lungs damage. This virus can infect both animals, and other people and its control are complicated because there's no effective vaccine or drugs available in markets for the treatments for COVID-19 so far. During this study, we docked some flavonoids against the target protein Mpro(6lu7) shows the binding energy between -8.68 kcal/mole to -6. 68 kcal/mol compared to native ligand (PRD_002214). The compounds Catechins, Luteoforol, Sappanchal-cone, Baicalein, Vitexin, Chrysosplenol, 5,6,7-Trimeth-oxyflavone, showed almost equal binding energy towards the native ligand except for Genistein. Our analyses revealed that the highest nine hits might function potential anti- SARS-CoV-2 lead molecules for further innovation and drug development process to combat COVID-19 also nearly as good drug-likeness properties studied supported the Lipinski's rules of 5.

*Corresponding Author

Name: Kaviarasu J
Phone:
Email: casureshkumar1985@gmail.com

eISSN: 2277-2782

DOI: https://doi.org/10.26452/ijntps.v10i2.1220

Production and Hosted by

ScienzTech.org

INTRODUCTION

Coronaviruses are an outsized family of viruses that are known to cause ailment starting from the cold to further severe diseases like Middle East Respiratory Syndrome (MERS) and Severe Acute Respiratory Syndrome (SARS). A unique coronavirus (COVID-19) was identified in 2019 in Wuhan, China. This is often a replacement coronavirus that has not been previously identified in humans.The onset of symptoms like fever, cough, fatigue, production of sputum, shortness of breath, pharyngitis, headache alongside some with reports of diarrhoea and vomiting began to increase because the group of pneumonia cases from December 2019 and later they were identified as β-coronavirus in Wuhan, Hubei Province, China [1]β-coronavirus was primarily named as 2019- novel coronavirus (2019-nCoV) on 12 January 2020 by WHO and formally named the disease as coronavirus 2019 (COVID-19) and as a world emergency disease of cause and concern globally, International Committee of Coronavirus Study Group (CSG) suggested the utilization of the name as SARS- CoV-2 which was published on 11 February 2020. [2]Currently, no specific antiviral treatment exists to defeat this illness that was previously ended by control measures, like travel restriction and patient isolation. In winter 2019 a replacement sort of pneumonia disease emerged in Wuhan, Hubei province (China). [3, 4] Ithad been called SARS-CoV-2 and rapidly spread from animals to humans. The diffusion in humans was very rapid. On 6^{th} June 2020, a complete of 6,976,045 confirmed infections were reported worldwide and recovered 3,411,784 with 392,802 deaths. [5, 6]

The World Health Organization (WHO) plan to con-

tain the spreading includes the reduction of human-to-human spreading by limiting the contact between individuals, thus preventing transmission amplification events and communicating critical risk information to all or any communities. [5]The outbreak of Coronavirus is increasing day by day everywhere on the planet. Brazil is another country that has been affected most after the USA, from the Coronavirus followed by Iran, the UK, Russia, India and Spain. Despite being declared as an epidemic disease for the planet by WHO, there are not any appropriate vaccines and antiviral drugs available on the market to stop and treat virus infection. On 17-03-2020, the USA reported starting vaccine trial against Coronavirus, but it'll take quite one year to be available. Therefore, it's an urgent demand to develop effective drugs for treatments of 2019-nCoV. The event of effective treatments will take months or years, which can hamper the control of this pandemic problem. Therefore, effective treatment or control mechanism is required to be developed to stop Coronavirus. [6]Although the diagnosis of COVID-19 is predicated on the amplification of the viral genome in real-time PCR with specific probes, the present treatment of affected individuals is restricted to a mix of a broad-spectrum of antiviral drugs. [7] However, in many cases, this pharmacological approach has proven to be ineffective.

The current methods of latest coronavirus treatment

A variety of the targets considering the inhibition of the RNA transcription, RNA modification, virus packaging enzymes, the capsid, and therefore the surface proteins assist the virus in diffusing into the cells and may be considered strategies to deactivate or prohibit the propagation of RNA virus in cells and tissues. The present methods of COVID-19 treatment are composed of the administration of medicine like Remdesivir, Chloroquine, Arbidol, and Favipiravir and approach like interferon therapy. Currently, studies are that specialize in further investigation of the biochemical materials that would inhibit the most proteases of the virus or the compounds that would inhibit the propagation rate of the virus within the cells. The plants provide an ultimate, natural source of enzyme and viral propagation inhibitors to be implicated as a treatment method of disorders caused by SARS-Cov and SARS-Cov-2. Fortunately, there's a substantial similarity between the SARS-Cov and SARS-Cov-2 virus which is entirely 80% identity and 96% similarity of the genome. it's been confirmed that the PLPro and 3CLPro of the SARS-Cov and SARS-Cov2 are conserved. [8] Additionally, it's observed that there's a 76.10% identity between the mentioned viruses. Supported, it's expected that the results of the studies about the SARS-Cov might imply for research within the SARS-Cov2 to a high degree.

Flavonoids are relatively common natural products widely existing in Plant. Flavonoids, including Genistein, catechins and so on, are shown to scale back the infection of a spread of viruses affecting humans and animals, including adenovirus, HSV, HIV, porcine reproductive and respiratory syndrome virus, and rotavirus. [9] Current results about the mechanisms of action underlying their antiviral properties suggest a mixture of effects on both the virus and therefore the host cell. Flavonoids are reported to affect virus binding, entry, replication, viral protein translation, the formation of certain virus envelope glycoprotein complexes and virus release. [9] They also affect the spread of host cell signalling processes, including induction of gene transcription factors and secretion of cytokines. [9] Although massive promising results were from *in vitro* experiments, a couple of *in vivo* results can partly confirm theirs *in vivo* efficacy. [10] Flavonoids possess antiviral properties against a wide range of viruses under both in vitro and *in vivo* conditions (Figures 1 and 2). [11]

In this study, we used enzymes; Mpro of virus-cell [12] as molecular targets against Coronavirus. SARS-CoV-2 may be a (+) SS RNA virus that encodes many structural and non-structural proteins. The Mpro may be a non-structural protein that cuts two replicase polyproteins leading to matured proteins that are required to mediate viral replication and transcription. during this way, by inhibition of the Mpro, we will stop virus replication in such how that it could block SARS-CoV-2 outbreak. [13, 14]Therefore, we selected Mpro, protease as a target to inhibit virus replication (SARS-CoV-2).

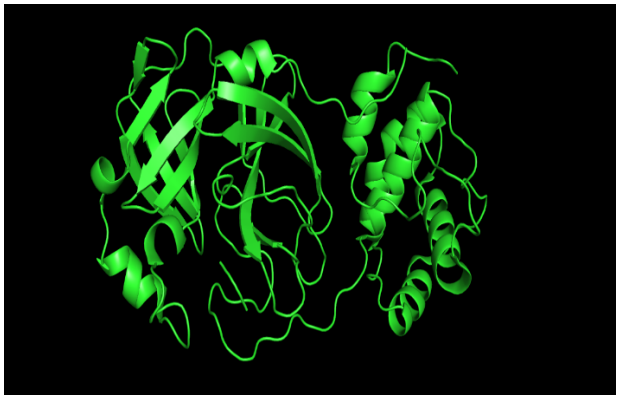

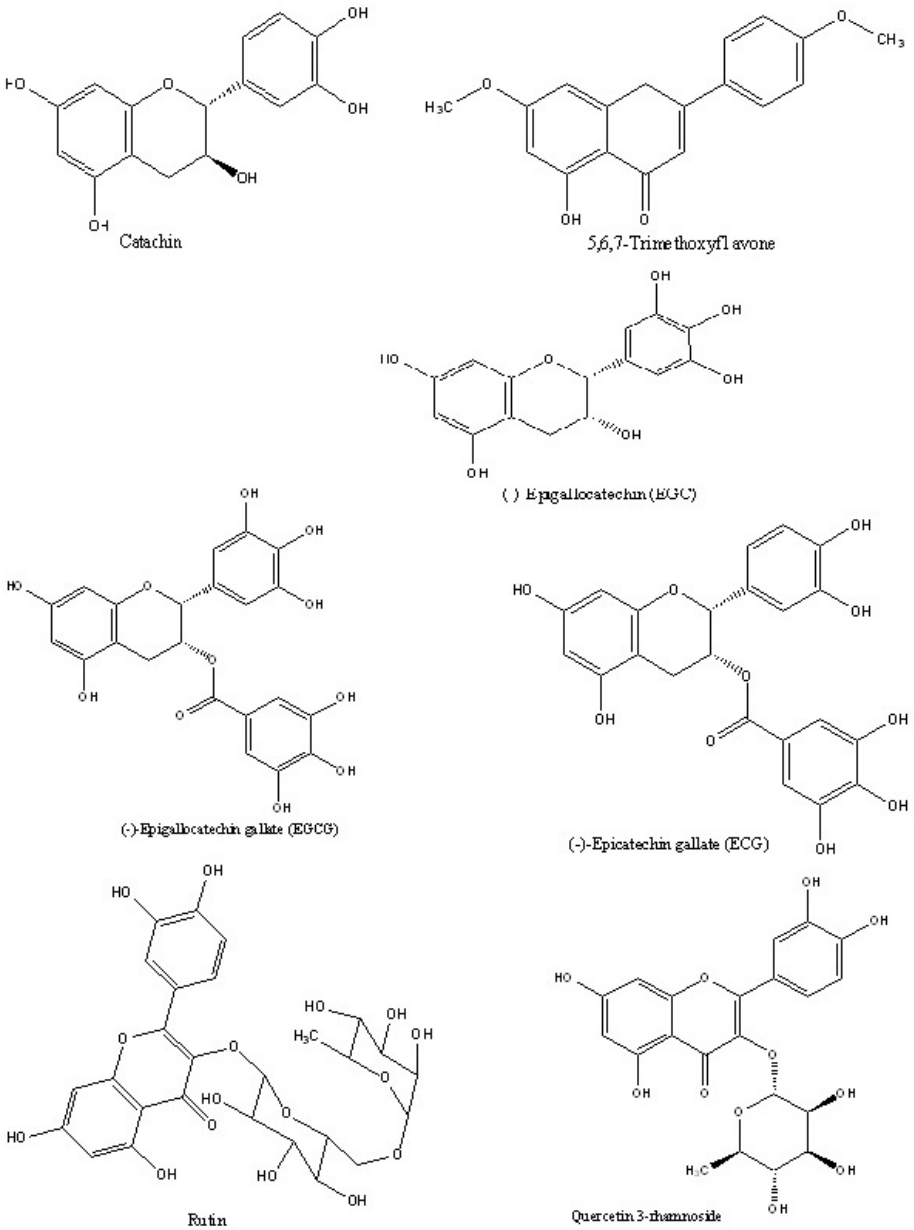

Figure 1: The chemical structures of some active flavonoids from Natural Products

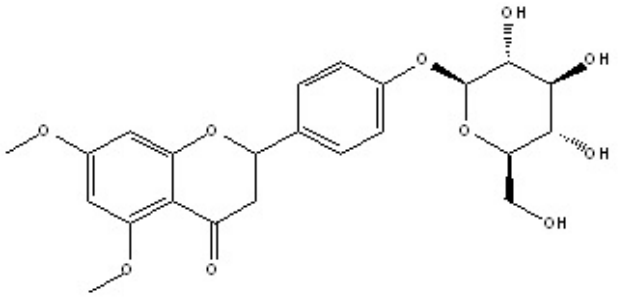

5,7-dimethoxyflavanone-4'-O-beta-d-glucopyranoside

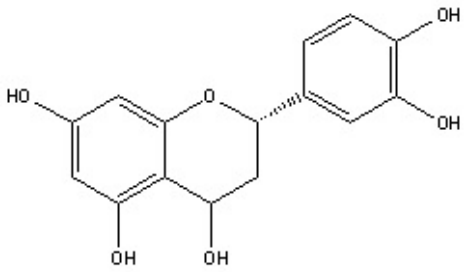

Lutecoforol

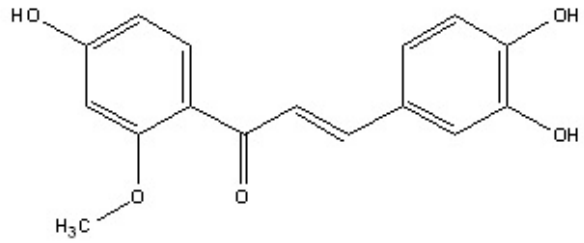

Sappanchalcone

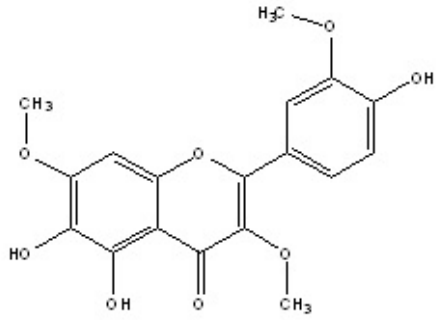

Chrysosplenol

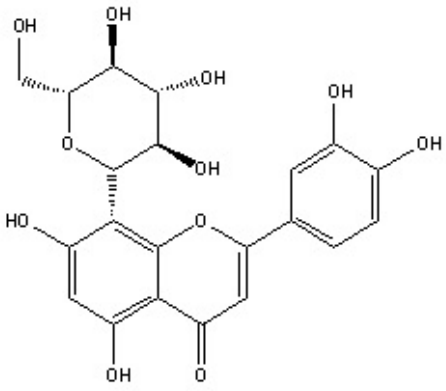

Orientin

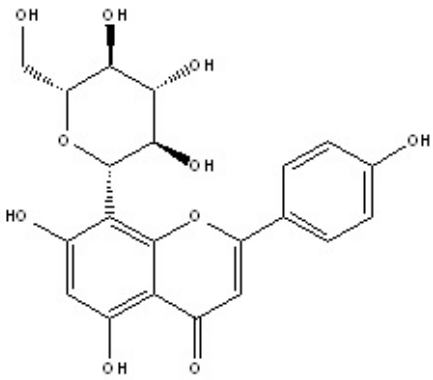

Vitexin

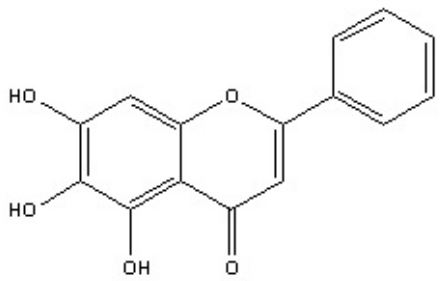

Baicalein

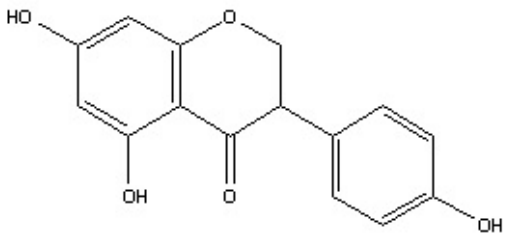

Genistein

Figure 2: The chemical structures of some active flavonoids from Natural Products

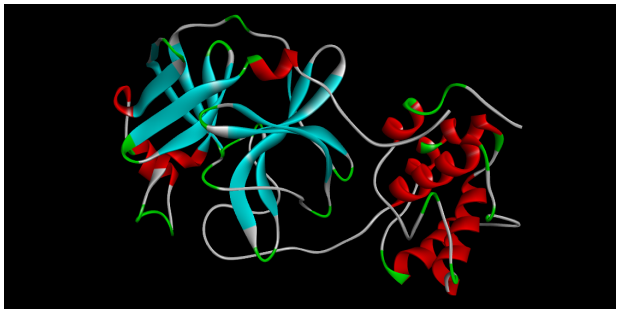

Figure 3: Chain-A Structure of 6LU7 viewed using PyMol and discovery studio.

MATERIALS AND METHODS:

Macromolecule structure retrieval: The structure of Mpro-PDB ID:6LU7 were retrieved from Protein Data Bank (PDB). [15]PDB is a database that contains the data of experimental structures of proteins and nucleic acids. Structure of 6LU7 was a homodimer (contain chain- A and chain-C). Only chain A was used for docking studies (Figure 3). All the other strings, water molecules, ions, and ligands were removed from the protein molecule using PyMOL. After that, the addition of polar hydrogen atoms to the receptor molecule was carried out by using MG Tools of AutoDock software 4.2. The structure of the protein was saved in PDB format for further analysis.

Ligand structure retrieval

Drug scan

All the fifteen ligands were verified their drug potential based on Lipinski's rule of five. Molinspiration has used for calculating Lipinski's properties. Lipinski's rule mainly governs the molecular characteristics, such as molecular weight, log P, the number of hydrogen bond acceptors, and several hydrogen bond donors. Any ligands showing violations of Lipinski's rule was rejected from further studies.

Active site prediction

The amino acids involved in active pocket development were determined using Computed Atlas for Surface Structure of proteins (CASTp). CASTp is a straightforward and useful web-based tool for determining the topology and active site pockets in the proteins. [16] The Active site determination is important to set the grid box at prior docking studies.

ADME/T prediction

Absorption, distribution, metabolism, excretion, and toxicity (ADMET) of the ligands and their pharmacokinetic properties are needed to be evaluated in their activity inside the body. The ADMET properties of the ligands were analyzed using admet SAR, an online ADMET prediction tool [17] .

Auto Docking and visualization: AutoDock 4.2 was used for Docking of ligands to the macromolecule. Auto Docking is the fully automated docking software tool; it is most broadly used to study the protein-ligand binding and interactions. Macromolecule was primarily fixed by adding polar hydrogen, Kollman charges. Ligand molecule was added to gasteiger charges. Autodock 4.2 allows setting a specific target site with the help of the grid box. The grid centre for Docking was set X= -12.71, Y= 17.14 and Z= 65.92 with dimensions of the grid box 40 $\times$ 40 $\times$ 40Å for 6LU7. The output for ligand conformations was analyzed using stochastic Lamarckian genetic algorithm. [18] The least negative ΔG indicates a strong binding and favourable formation for the ligand and the protein interaction. [19]The 3D visualization of docked structures was accomplished using Discovery studio [20] . Protein-ligand interactions, structure and ligand designing are few facilities available in Discovery studio. [21]

RESULT AND DISCUSSION

A new coronavirus, known as severe acute respiratory syndrome coronavirus-2 (SARS-CoV-2), is the etiological agent responsible for the 2019-2020 viral pneumonia outbreak of coronavirus disease 2019 (COVID-19). Currently, there are no targeted therapeutic agents for the treatment of this disease. At this time, we describe the results of docking study of the target main protease (Mpro) of SARS-CoV-2: Mpro is a crucial enzyme of coronaviruses (PDB ID: 6LU7) with screened nine plant flavonoids compounds to inhibit 6LU7.

For in silico analysis of plant-derived flavonoid compounds, the drug potential of all the ligands was tested using Lipinski's rule of five. Molinspiration server was used to analyze the molecular parameters of the ligands. The results include the molecular weight, numbers of hydrogen donors, acceptors, and lipophilicity of the ligand molecules. Out of 15 compounds studied, nine compounds were obeyed Lipinski's rule of five, except Epigallocatechin gallate (EGCG), Epicatechin gallate (ECG), Epigallocatechin (EGC), Rutin, Orientin, Quercetin 3-rhamnoside (Q3R), which exhibited More than one violation; hence, these compounds were rejected from further analysis. Log p-value indicates the hydrophilic and hydrophobic nature of the ligands. Only Rutin had negative log p score indicating that these compounds are highly hydrophilic; the result is shown in (Table 1).

Active site pockets in 6LU7 were determined using CASTp. CASTp is a web-based tool to assess the

Figure 4: Amino acids involved in forming an active site for 6lu7. Letters highlighted in blue colour indicates the active site residues.

amino acid residues in the pocket region of the proteins. CASTp results are represented in Figure 4 for 6LU7. From CASTp results, only the amino acids in the active site and their positions are listed as (Table 2) for 6LU7.

The ADMET properties of the ligands are required to be known for determining their drug likeliness. ADMET properties of the compounds in the study were analyzed using admet SAR. All the compounds showed good human gastrointestinal absorption (GIA), blood-brain barrier (BBB) penetration. No drug was carcinogenic. The results of GIA, BBB penetration, caco$_2$, acute toxicity, Log S, hepatotoxicity values for the compounds are listed in (Table 3).

Autodock4.2 were used for performing docking analysis for above selected nine compounds and their binding potential with 6LU7 was analyzed. The binding energy, number of hydrogen bond interactions, and amino acids involved in the interactions are tabulated in (Table 4) and the Interacting residues, hydrogen bond, length and other residues of ligand showed in (Table 5).

The binding energy of ligand PRD_002214(R) with the target is -7.37kc/mol. The torsional energy of PRD_002214 was +5.37 kc/mol. This ligand has intermolecular energy of -12.74 with a total internal of -5.60. The unbounded energy of this ligand is -5.60, and the inhibition constant is 3.97 μm. The Docking of this ligand with 6LU7 has seven interacting residues at the binding site which are GLU 16, ASN 142, GLN 189, MET 49, GLN 189, MET 165, LEU 141, MET 49 and HIS 41. Ligand PRD_002214 exhibited four hydrogen bond interactions with an amino acid in the active site are shown in Figure 5. The hydrogen bond is formed between the amino group of the active site with the ligand and higher hydrogen bond distance of 3.21Å.

The binding energy of ligand Catechins with the target is -7.89kc/mol. The torsional energy of Catechins was +1.79 kc/mol. This ligand has intermolecular energy of -9.68 with a total internal of -1.05. The unbounded energy of this ligand is -1.05, and the inhibition constant is 1.64 μm. The Docking of this ligand with 6LU7 has nine interacting residues at the binding site which are GLN 192, THR 190, GLU 166, HIS 164, ASP 187, TYR 54, HIS 41, MET 165, MET 49. Ligand Catechins exhibited six hydrogen bond interactions with an amino acid in the active site are shown in Figure 6. The hydrogen bond is formed between the amino group of the active site with the ligand and higher hydrogen bond distance of 2.38Å.

The binding energy of ligand Sappanchalcone with the target is -7.63kc/mol. The torsional energy of Sappanchalcone was +2.09 kc/mol. This ligand has intermolecular energy of -9.72 with a total internal of -1.51. The unbounded energy of this ligand is -1.51, and the inhibition constant is 2.55 μm. The Docking of this ligand with 6LU7 has eight interacting residues at the binding site which are TYR 54, GLU 166, THR 190, ASP 187, PRO 168, ARG 188, HIS 41, MET165, LEU 167, GLN 189. Ligand Sappanchalcone exhibited three hydrogen bond interactions with an amino acid in the active site are shown in Figure 7. The hydrogen bond is formed between the amino group of the active site with the ligand and hydrogen bond distance of 2.32Å.

The binding energy of ligand Luteoforol with the target is -7.36kc/mol. The torsional energy of Luteoforol was +1.79 kc/mol. This ligand has intermolecular energy of -9.05 with a total internal of -2.53. The unbounded energy of this ligand is -2.53, and the inhibition constant is 4.77 μm. The Docking of this ligand with 6LU7 has five interacting residues at the binding site, which are HIS 163, HIS 164, THR 190, MET 165, CYS 145. Ligand Luteoforol exhibited five hydrogen bond interactions with an amino acid

Table 1: Lipinski's properties of Flavonoid compounds analyzed using molinspiration

S. No	Compound	Molecular weight (<500 Da) g/mol	Log P (<5)	H-bond donor (5)	H-bond acceptor (<10)	No. of violations
	PRD_002214	680.79	3.73	5	9	2
1	Catechins	290.27	1.37	5	6	0
2	Epigallocatechin gallate (EGCG)	**458.37**	**2.25**	**8**	**11**	**2**
3	Epicatechin gallate (ECG)	**442.37**	**2.25**	**7**	**10**	**1**
4	Epigallocatechin (EGC)	**306.27**	**1.08**	**6**	**7**	**1**
5	5,6,7-Trimethoxyflavone	312.32	3.54	0	5	0
6	Sappanchalcone	286.28	2.35	3	5	0
7	Luteoforol	290.27	1.28	5	6	0
8	Rutin	**610.52**	**-1.06**	**10**	**16**	**3**
9	Genistein	270.24	2.27	3	5	0
10	Baicalein	270.24	2.68	3	5	0
11	Orientin	**448.38**	**0.03**	**5**	**11**	**2**
12	Vitexin	150.22	3.34	1	1	0
13	Chrysosplenol	360.69	2.31	3	8	0
14	Quercetin 3-rhamnoside (Q3R)	**448.38**	**0.64**	**7**	**11**	**2**
15	5,7-dimethoxyflavanone-4'-O-beta-d-glucopyranoside	462.45	0.59	4	10	0

Table 2: List of amino acids in the active site pocket of 6lu7 obtained from CASTp

Amino acids	position	Amino acids	position
Threonine	24	Leucine	141
Threonine	25	Asparagine	142
Threonine	26	Glycine	143
Leucine	27	Serine	144
Histidine	41	Cysteine	145
Threonine	45	Histidine	163
Serine	46	Methionine	165
Methionine	49	Glutamine	166
Phenylalanine	140	Histidine	172

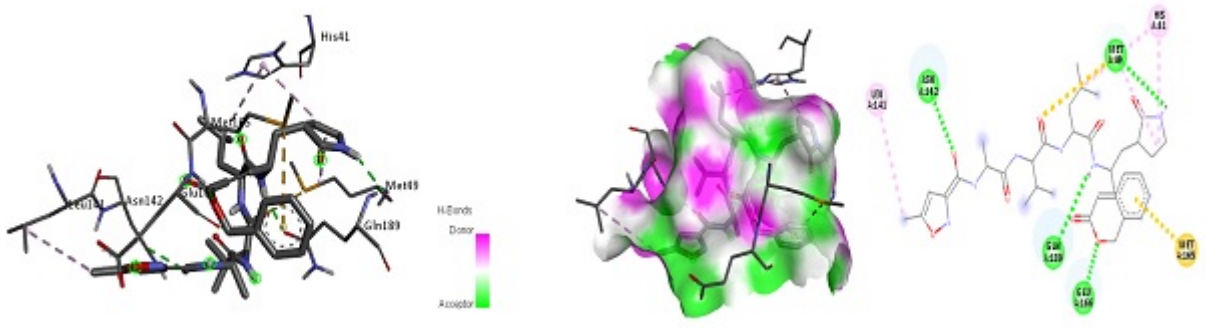

Figure 5: Docking studies of PRD_002214 with the target protein (2D and 3D view)

Table 3: ADMET properties of screened phytochemicals.

S. No	Compound	BBB	GIA	Caco$_2$	Acute toxicity kg/mol	Carcinogens	Log s	hepatotoxicity
	PRD_002214	-	low	-	2.914	NC	-3.068	
1	Catechins	-	High	-	2.141	NC	-3.101	-
2	Sappanchalcone	+	High	+	2.203	NC	-2.779	+
3	Luteoforol	-	High	+	2.699	NC	-3.322	+
4	Genistein	-	High	+	1.842	NC	-3.093	+
5	Baicalein	-	High	-	1.887	NC	-2.999	+
6	Vitexin	-	Low	-	2.835	NC	-2.398	+
7	Chrysosplenol	-	High	+	2.645	NC	-3.512	+
8	5,6,7-Trimethoxy-flavone	-	High	+	2.135	NC	-3.867	+
9	5,7-dimethoxyflavan-one-4'-O-beta-d-glucopyranoside	-	Low	-	2.991	NC	-3.068	+

*BBB- Blood-Brain Barrier, GIA- Gastrointestinal Absorption, Caco2- Caco-2 Permeability, NC- Non-Carcinogens, (-) Negative, (+) Positive

Table 4: Docking result of ligands.

S. No	Compound	Binding energy (kcal/mol]	Inhibition energy/ ki	Torsional energy (kcal/mol]	Intermole. Energy (kcal/mol]	Total internal energy	Unbounded energy (kcal/mol)
	PRD_002214 (R)	-7.37	3.97 μm	+5.37	-12.74	-5.60	-5.60
1	Catechins	- 7.89	1.64 μm	+1.79	-9.68	-1.05	-1.05
2	Sappanchalcone	-7.63	2.55 μm	+2.09	-9.72	-1.51	-1.51
3	Luteoforol	-7.26	4.77 μm	+1.79	-9.05	-2.53	-2.53
4	Genistein	-6.38	21.03 μm	+1.19	-7.57	-0.82	-0.82
5	Baicalein	-7.28	4.58 μm	+1.19	-8.48	-2.11	-2.11
6	Vitexin	-7.55	2.90 μm	+2.98	-10.54	-5.02	-5.02
7	Chrysosplenol	-7.93	1.53 μm	+2.09	-10.02	-2.31	-2.31
8	5,6,7-Trimethoxy-flavone	-7.42	3.61 μm	+1.19	-8.62	-0.88	-0.88
9	5,7-dimethoxyflavan-one-4'-O-beta-d-glucopyranoside	-8.68	430.93 μm	+2.68	-11.37	-2.72	-2.72

Table 5: Interacting residues, hydrogen bond, length and other residues of the ligand.

Ligand	No. of hydrogen bond	H-bond interaction residues	H-bonds distance (A°)	Oher interacting residues
PRD_002214(R)	2	GLU 66ASN 142GLN 189MET 49	1.73 3.21 3.04 2.18	MET 165, LEU 141, HIS 41
Catechins	6	GLN 192 THR 190 GLU 166 HIS 164 ASP 187 THR 190	2.771.81 2.38 2.30 2.18 2.22	HIS 41, MET 165, MET 49
Sappanchalcone	3	GLU 166 THR 190 ASP 187	2.26 1.84 2.32	MET 165, CYS 145
Luteoforol	5	HIS 163 HIS 164 THR 190 THR190 HIS164	2.412.25 1.80 2.46 2.41	GLN 18, MET 165, CYS 145
Genistein	6	SER 144 CYS 145 HIS 163 THR 26 LEU 144GLU 166	2.662.722.041.99 3.48 2.10	ASN 142, HIS 41, LEU 27
Baicalein	3	GLU 166 THR 190 GLU 166	2.10 2.11 3.01	ARG 188, GLN 189, HIS 41, ASP 187, MET 165, MET 49
Vitexin	5	ASP 187CYS 145THR190 TYR 190 GLU166	4.70 4.82 4.26 3.64 3.82	CYS44, HIS 41, MET165, MET49
Chrysosplenol C	2	GLU 166 THR 190	1.94 2.09	MET 165, PRO 168, PRO 52, ARG 188, ARG 187, MET 49
5,6,7-Trimethoxy-flavone	3	GLU 166 GLU 166 GLY 148	3.05 2.19 2.08	MET 49, HIS 145, CYS 44, HIS 163
5,7-dimethoxyflavan-one-4'-O-beta-d-glucopyranoside	9	GLN 192 HIS 163 LUE 141 LUE 141 GLY 143 SER 144 CYS 145 CYS 145 CYS 145	2.86 1.63 2.16 2.11 2.22 2.05 2.33 2.17 3.21	MET 165, GLN 189, HIS 41

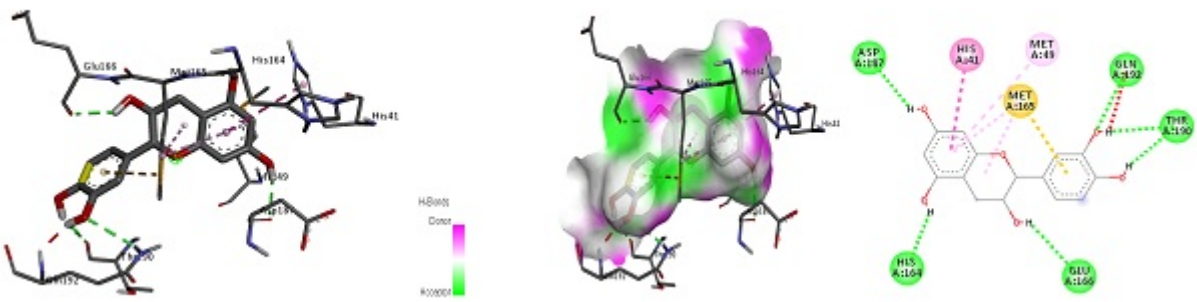

Figure 6: Docking studies of catechins with the target protein (2D and 3D view)

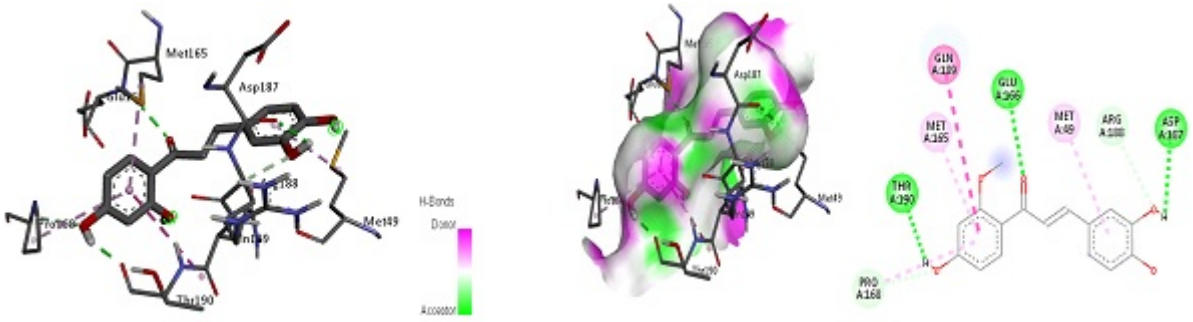

Figure 7: Docking studies of Sappanchalcone with the target protein (2D and 3D view).

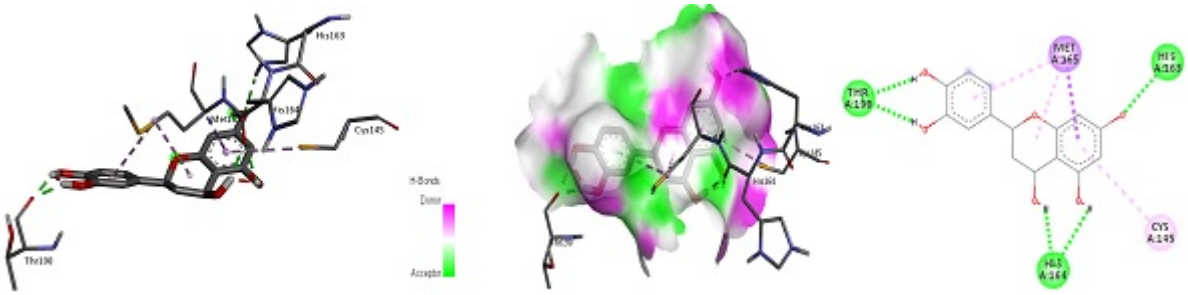

Figure 8: Docking studies of Luteoforol with the target protein (2D and 3D view).

in the active site are shown in Figure 8. The hydrogen bond is formed between the amino group of the active site with the ligand and hydrogen bond distance of 2.46Å.

The binding energy of ligand Genistein with target is-6.38kc/mol. The torsional energy of Genistein was +1.19 kc/mol. This ligand has intermolecular energy of -7.57 with a total internal of -0.82. The unbounded energy of this ligand is -0.82, and the inhibition constant is 21.03 μm. The Docking of this ligand with 6LU7 has nine interacting residues at the binding site which are SER144, CYS145, HIS163, THR26, GLU166, LEU 141, ASN 142, HIS 41, LEU 27. Ligand Genistein exhibited six hydrogen bond interactions with an amino acid in the active site are shown in Figure 8. The hydrogen bond is formed between the amino group of the active site with the ligand and hydrogen bond distance of 3.48Å.

The binding energy of ligand Baicalein with the target is -7.28kc/mol. The torsional energy of Baicalein was +1.19 kc/mol. This ligand has intermolecular energy of -8.48 with a total internal of -2.11. The unbounded energy of this ligand is -2.11, and the inhibition constant is 4.58 μm. The Docking of this ligand with 6LU7 has eight interacting residues at the binding site which are GLU 166, THR 190, ARG 188, GLN 189, HIS 41, ASP 187, MET 165, MET 49. Ligand Baicalein exhibited three hydrogen bond interactions with an amino acid in the active site are shown in Figure 10. The hydrogen bond is formed between the amino group of the active site with the ligand and higher hydrogen bond distance of 3.01Å.

The binding energy of ligand Vitexin with the target is -7.55kc/mol. The torsional energy of Vitexin was +2.98kc/mol. This ligand has intermolecular energy of -10.54 with a total internal of -5.02. The unbounded energy of this ligand is -5.02, and the inhibition constant is 2.90 μm. The Docking of this ligand with 6LU7 has eight interacting residues at the binding site which are ASP 187, CYS 145, TYR 190, CYS44, HIS 41, MET165, MET49, GLU166. Ligand Vitexin exhibited five hydrogen bond interactions with an amino acid in the active site are shown in Figure 11. The hydrogen bond is formed between the amino group of the active site with the ligand and higher hydrogen bond distance of 4.82Å.

The binding energy of ligand Chrysosplenol C with the target is -7.93kc/mol. The torsional energy of Chrysosplenol C was +2.09kc/mol. This ligand has an intermolecular power of -10.02 with a total internal of -2.31. The unbounded energy of this ligand is -2.31, and the inhibition constant is 1.53 μm. The Docking of this ligand with 6LU7 has eight interacting residues at the binding site which are GLU 166, THR 190, MET 165, PRO 168, PRO 52, ARG 188, ARG 187, MET 49. Ligand Chrysosplenol C exhibited two hydrogen bond interactions with an amino acid in the active site are shown in Figure 12. The hydrogen bond is formed between the amino group of the active site with the ligand and higher hydrogen bond

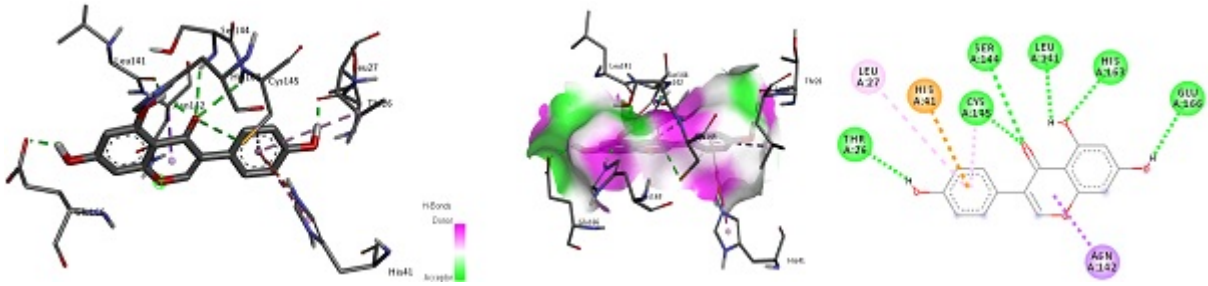

Figure 9: Docking studies of Genistein with the target protein (2D and 3D view)

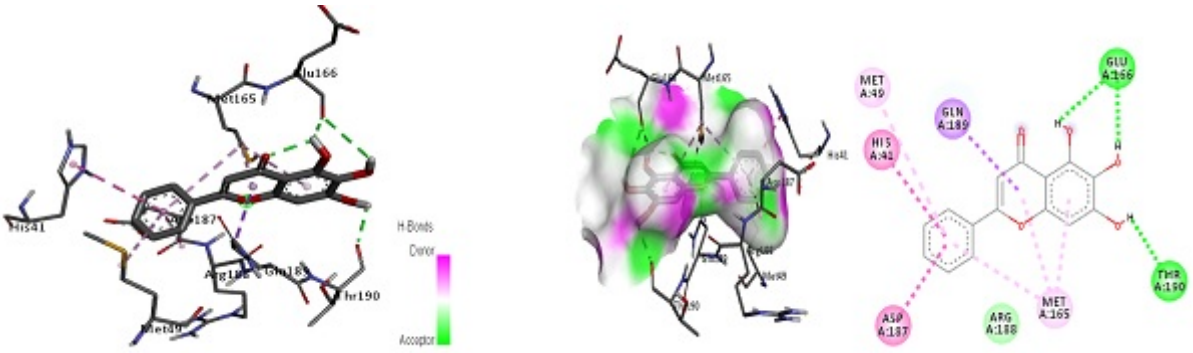

Figure 10: Docking studies of Baicalein with the target protein (2D and 3D view).

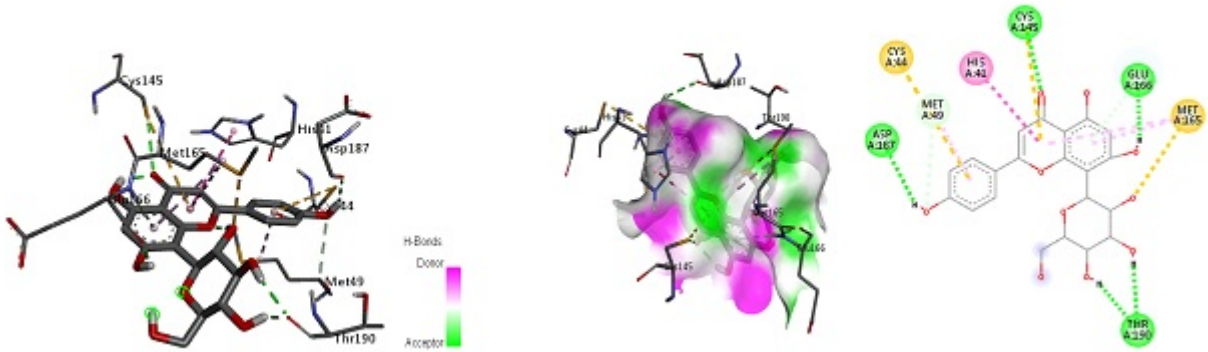

Figure 11: Docking studies of Vitexin with the target protein (2D and 3D view).

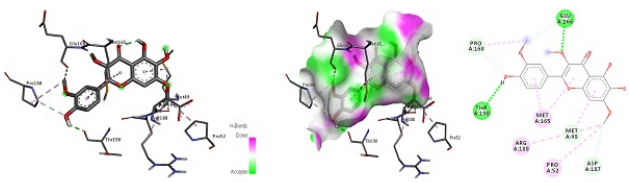

Figure 12: Docking studies of Chrysosplenol C with the target protein(2D and 3D view).

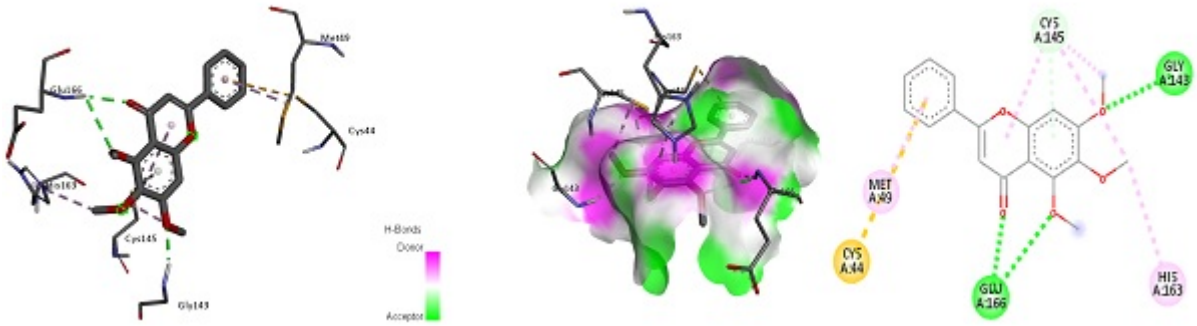

Figure 13: Docking studies of 5,6,7-Trimethoxyflavone with the target protein (2D and 3D view).

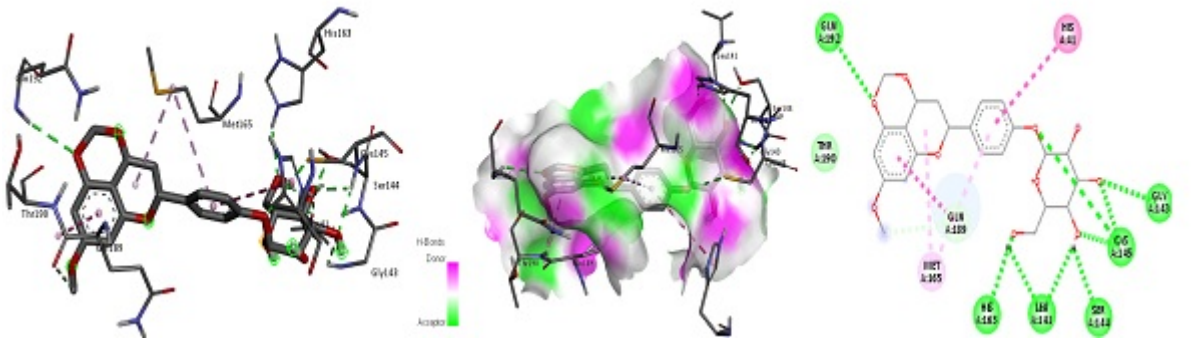

Figure 14: Docking studies of 5,7-dimethoxyflavan-one-4'-O-beta-d-glucopyranoside & the target protein (2D and 3Dview). |

distance of 2.09Å.

The binding energy of ligand 5,6,7-Trimethoxyflavone with the target is -7.42kc/mol. The torsional strength of 5,6,7-Trimethoxyflavone was +1.19kc/mol. This ligand has an intermolecular power of -8.622 with a total internal of -0.88. The unbounded energy of this ligand is -0.88, and the inhibition constant is 3.61 μm. The Docking of this ligand with 6LU7 has seven interacting residues at the binding site which are GLU 166, GLY 148, MET 49, HIS 145, CYS 44, HIS 163. Ligand 5,6,7-Trimethoxy-flavone exhibited three hydrogen bond interactions with an amino acid in the active site are shown in Figure 13. The hydrogen bond is formed between the amino group of the active site with the ligand and hydrogen bond distance of 3.05Å.

The binding energy of ligand 5,7-dimethoxyflavan-one-4'-O-beta-d-glucopyranoside with the target is -8.68kc/mol. The torsional energy of 5,7-dimethoxyflavan-one-4'-O-beta-d-glucopyranoside was +2.68kc/mol. This ligand has an intermolecularμ energy of -11.37 with a total internal of -2.72. The unbounded energy of this ligand is -2.72, and the inhibition constant is 430.93 μm. The Docking of this ligand with 6LU7 has nine interacting residues at the binding site which are GLN 192, HIS 163, LUE 141, GLY 143, SER 144, CYS 145, MET 165, GLN 189, HIS 41. Ligand 5,7-dimethoxy-flavan-one-4'-O-beta-d-glucopyranoside exhibited nine hydrogen bond interactions with an amino acid in the active site are shown in Figure 14. The hydrogen bond is formed between the amino group of the active site with the ligand and hydrogen bond distance of 3.21Å.

CONCLUSION

In silico molecular Docking, simulation Study was performed, and it was found that all the test compounds are binding with the target main protease (Mpro) of SARS-CoV-2, very efficiently as compare with native ligand (PRD_002214). When the receptor (6LU7) was docked with 5,7-dimethoxyflavan-one-4'-O-beta-d-glucopyranoside, the energy value obtained was (-8.68 kcal /mol) using Autodock 4.2. When Genistein was docked against the same receptor, it was (-6.68 kcal /mol). Thus, we conclude that all these flavonoids can be utilized as potential antiviral candidates for the treatment of coronavirus. These novel molecules could be used for further innovation and development of antiviral compounds against Coronavirus/SARS-CoV-2.

FUNDING SUPPORT

None

ACKNOWLEDGEMENT

The authors are thankful to all who have extended their constant support for the completion of the work.

Conflict of Interest

Authors declared no conflict of interest.

REFERENCES

[1] Guan WJ, Ni ZY, Hu Y, Liang WH, Ou CQ, He JX, et al. Clinical characteristics of Coronavirus disease 2019 in China. Medical Treatment Expert Group for Covid. 2020;p. 19–19.

[2] Guo Y, Cao Q, Hong Z, Tan Y, Chen S, Jin H, et al. The origin, transmission and clinical therapies on coronavirus disease 2019 (COVID-19) outbreak - an update on the status. Military Medical Research. 2020;7(1):11–11.

[3] Wang Y, Wang Y, Chen Y, Qin Q. Unique epidemiological and clinical features of the emerging 2019 novel coronavirus pneumonia (COVID-19) implicate special control measures. J Med Virol. 2020;.

[4] Zhu ZB, Zhong CK, Zhang KX, Dong C, Peng H, Xu AL, et al. Epidemic trend of corona virus disease 2019 (COVID-19) in mainland China. Zhonghua Yu Fang Yi Xue Za Zhi. 2020;54:22–22.

[5] World Health Organization. Coronavirus Disease 2019 (COVID-19) Situation Report –43. 2020. ;.

[6] Zhang DH, Wu KL, Zhang X, Deng SQ, Peng B. In silico screening of Chinese herbal medicines with the potential to directly inhibit 2019 novel coronavirus. J Integr Med. 2020;18:152–158.

[7] Xu J, Shi PY, Li H, Zhou J. Broad Spectrum Antiviral Agent Niclosamide and Its Therapeutic Potential. ACS Infect Dis. 2020;6(5):909–915.

[8] Yonesi M, Rezazadeh A. Plants as a Prospective Source of Natural Anti-viral Compounds and Oral Vaccines Against COVID-19 Coronavirus. Preprints 2020. 2020;Available from: 10.20944/preprints202004.0321.v1.

[9] Andres A, Donovan SM, Kuhlenschmidt MS. Soy isoflavones and virus infections. The Journal of Nutritional Biochemistry. 2009;20(8):563–569. Available from: 10.1016/j.jnutbio.2009.04.004.

[10] Miki K, Nagai T, Suzuki K. Anti-influenza virus activity of biflavonoids. Bioorg Med Chem Lett. 2007;17:772–775.

[11] Liu AL, Du GH. Antiviral Properties of Phytochemicals Chapter;(3).

[12] de Wit E, van Doremalen N, Falzarano D, Munster VJ. SARS and MERS: recent insights into emerging coronaviruses. Nature Reviews Microbiology. 2016;14(8):523–534. Available from: 10.1038/nrmicro.2016.81.

[13] Du L, He Y, Zhou Y, Liu S, Zheng BJ, Jiang S. The spike protein of SARS-CoV–a target for vaccine and therapeutic development. Nat Rev Microbiol. 2009;7:226–236.

[14] Towler P, Staker B, Prasad SG, Menon S, Tang J, Parsons T, et al. ACE2 X-Ray Structures Reveal a Large Hinge-bending Motion Important for Inhibitor Binding and Catalysis. Journal of Biological Chemistry. 2004;279(17):17996–18007. Available from: 10.1074/jbc.m311191200.

[15] Huang YH, Rose PW, Hsu CN. Citing a data repository: a case study of the protein data bank. PloS one. 2015;10(8):136631–136631.

[16] Lipinski CA, Lombardo F, Dominy BW, Feeney PJ. Experimental and computational approaches to estimate solubility and permeability in drug discovery and development settings. Advanced Drug Delivery Reviews. 2012;64:4–17. Available from: 10.1016/j.addr.2012.09.019.

[17] Cheng F, Li W, Zhou Y, Shen J, Wu Z, Liu G, et al. admetSAR: a comprehensive source and free tool for assessment of chemical ADMET properties. J Chem Inf Model. 2012;p. 3099–105.

[18] Hari S. In silico Molecular Docking and ADME/T analysis of plant compounds against IL17A and IL18 targets in gouty arthritis. Journal of Applied Pharmaceutical Science. 2019;9(07):18–026.

[19] Afriza D, Suriyah WH, Ichwan SJA. In silicoanalysis of molecular interactions between the anti-apoptotic protein survivin and dentatin, nordentatin, and quercetin. Journal of Physics: Conference Series. 2018;1073(3):032001–032001. Available from: 10.1088/1742-6596/1073/3/032001.

[20] Kemmish H, Fasnacht M, Yan L. Fully automated antibody structure prediction using BIOVIA tools: Validation study. PLOS ONE.

2017;12(5):e0177923–e0177923. Available from: 10.1371/journal.pone.0177923.

[21] Meenambiga SS, Venkataraghavan R, Biswal RA. In silico analysis of plant phytochemicals against secreted aspartic proteinase enzyme of Candida albicans. J Appl Pharm Sci. 2018;8(11):140–50.

Cite this article: Kaviarasu J, CA Suresh Kumar, N Naimuddeen. ***In silico*** **molecular docking studies and ADME/T analysis of Some Flavonoids against the target of Mpro in COVID-19**. Int. J Nov. Tren. Pharm. Sci. 2020; 10(2): 33-46.